Detection of gold nanoparticles using an immunoglobulin-coated piezoelectric sensor

2008 Nanotechnology 19 495502

(http://iopscience.iop.org/0957-4484/19/49/495502)

Nanotechnology **19** (2008) 495502 (6pp) doi:10.1088/0957-4484/19/49/495502

Detection of gold nanoparticles using an immunoglobulin-coated piezoelectric sensor

Yu-Shiun Chen[1,2], Yao-Ching Hung[3], Kaochao Chen[1] and Guewha Steven Huang[1,4]

[1] Institute of Nanotechnology, National Chiao Tung University, 1001 University Road, EE137, Hsinchu 300, Taiwan, Republic of China
[2] Institute of Materials Science and Engineering, National Chiao Tung University, 1001 University Road, EE137, Hsinchu 300, Taiwan, Republic of China
[3] Section of Gynecologic Oncology, Department of Obstetrics and Gynecology, China Medical University, 91 Hsueh Shih Road, Taichung 404, Taiwan, Republic of China

E-mail: gstevehuang@mail.nctu.edu.tw

Received 12 May 2008, in final form 14 October 2008
Published 18 November 2008
Online at stacks.iop.org/Nano/19/495502

Abstract
Since the existence of nanoparticles in our environment has already attracted considerable attention due to their possible toxic impact on biological systems, the field detection of nanoparticles is becoming a technology that will be much in need. We have constructed a piezoelectric sensor with an antibody-coated electrode. The antiserum can bind gold nanoparticles with a high degree of selectivity and sensitivity. The biosensor thus constructed can detect 4, 5, or 6 nm gold nanoparticles (GNPs) depending on the coated antiserum. The sensitivity for the detection of 5 nm GNPs was 10.3 ± 0.9 ng Hz^{-1}, with the low limit of detection at 5.5 ng. A quartz crystal microbalance (QCM) sensor was capable of detecting GNPs and other types of nanoparticle, such as ZnO, or Fe_3O_4. The current study provides, for the first time, a platform for detecting nanoparticles in a convenient, economical manner.

1. Introduction

Nanosized particles have received considerable interest in the past two decades. This is in part due to the special properties and the toxicity attained when substances are reduced to the nanoscale. However, a wide distribution of sizes gives rise to major limitations for precise investigation of their unique physical and chemical characteristics. In particular, the detection of nanosized particles has brought considerable attention to many scientific areas.

A number of methods have been developed for analyzing nanoparticles, for example, light scattering [1], optical absorbance [2–8], plasmon absorption [9–11], spectral and surface plasmon resonance (SPR) [12–17], surface-enhanced Raman scattering (SERS) [18–21], electrical and electrochemical signals [22, 23], and electron microscopy (transmission electron microscopy (TEM) and scanning electron microscopy (SEM)). The sensitivity varies from mM (for electrical and electrochemical signals) to pM (for SPR). However, the selectivity is generally poor for most methods. Because samples have to be purified to a stringent degree before analysis, most of these methods are not suitable for the detection of nanoparticles from the environment.

Biological interaction is characterized by high selectivity of both surface chemistry and physical shape. Antibody–antigen recognition has been applied as a standard detecting tool; however, there is no report of using antibodies to detect nanoparticles, so far. This is probably because nanoparticles in general are not a good substrate with which to simulate an immune response. Previously, we have shown that the ability of gold nanoparticles to stimulate an immune response depends on the size of the particles [24]. Thus, if the size is controlled it is possible to obtain antibodies for the detection of nanoparticles.

A quartz crystal microbalance (QCM) is a mass-detection device that operates based on the piezoelectric properties of

[4] Author to whom any correspondence should be addressed.

quartz crystals [25]. The QCM is unsophisticated and cost-effective, has real-time response and high resolution, and is stable. Because of their extraordinary sensitivity and stability, QCMs have been applied in recent years as biosensors for the real-time detection of biomolecules.

The purpose of this study is to demonstrate the possibility of using an antibody-coated QCM to detect gold nanoparticles. The sensitivity of the antibody-coated QCM indicated that using this type of detection is very economical, convenient, and accurate.

2. Experimental details

2.1. Materials

An oscillator (Catalog #35366-10) and flow cell (Catalog #35363) were purchased from International Crystal Manufacturing Co. (Oklahoma City, USA). The QCM was fabricated from a 0.2 mm thick AT-cut quartz wafer. A laboratory-constructed transistor–transistor logic integrated circuit (TTL-IC) was used to power the QCM. An Agilent HP 53132 universal frequency counter was used to monitor the frequency output.

2.2. Preparation and characterization of gold nanoparticles

Seed colloids were prepared by adding 1 ml of 0.25 mM $HAuCl_4$ to 90 ml of H_2O and stirring for 1 min at 25 °C [26, 27]. Then 2 ml of 38.8 mM sodium citrate were added to the solution, which was stirred for 1 min, followed by the addition of 0.6 ml freshly prepared 0.1 M $NaBH_4$ in 38.8 mM sodium citrate. Different diameters of gold nanoparticles ranging from 2 to 12 nm were generated by adjusting the volume of sodium citrate, seed colloid, and reaction temperature. The solution was stirred for an additional 5–10 min at 0–4 °C. The reaction temperature and reaction time were adjusted to obtain GNPs of larger size. All synthesized GNPs were characterized by UV absorbance and examined with electron microscopy (EM) and atomic force microscopy (AFM) for size and homogeneity.

2.3. Generation of antisera against GNPs

GNPs ranging from 4 to 6 nm in size were synthesized, purified by size-exclusion chromatography, and resuspended in phosphate-buffered saline before immunization. GNPs were emulsified thoroughly with complete adjuvant and injected peritoneally and weekly to BALB/C mice. Antiserum was obtained after four weeks. The binding activity of antiserum against 5 nm GNPs was validated by an enzyme-linked immunosorbent assay (ELISA). Competition ELISA was performed to validate the binding specificity of antiserum using 5 nm GNPs and 5 nm ZnO as competitors. The binding activity was blocked in the presence of 5 nm GNPs but was undisturbed in the presence of 5 nm ZnO.

2.4. ELISA

Each microwell of a 96-well Corning plate was pretreated with 100 μl 2% 3-aminopropyltriethoxysilane (APTES) in ethanol for 20 min at room temperature followed by phosphate-buffered saline (PBS) washing. 150 μl of 15 mM GNPs were added to the microwells and incubated for 2 h at room temperature followed by Milli-Q water washing three times and then washing with 0.5% Triton X-100 in PBS three times. Blocking for nonspecific binding was performed by adding 100 μl of 3% BSA and incubating for 60 min at room temperature, followed by PBS washing three times. Binding was performed by adding 100 μl properly diluted antiserum into the microwells and incubating for 1 h at room temperature followed by thorough washes. Horseradish peroxidase (HRP)-conjugated anti-mouse IgG, 2,2′-azino-bis (3-ethylbenzthiazoline-6-sulfonic acid) (ABTS), and H_2O_2 were incorporated in sequence to the wells according to the manufacturer's protocol, and the binding efficiency was monitored by absorbance at 405 nm. The competition ELISA was performed in an Eppendorf tube by adding concentrated competitor to the anti-5 nm GNP antiserum in a total volume of 100 μl, incubated 1 h at room temperature, and used as antiserum following the previously described ELISA procedure [28, 29].

2.5. Cross-linking of immunoglobulin on to the QCM electrode

The gold electrode was cleaned by immersing in 1.2 M NaOH for 20 min, 1.2 M HCl for 5 min, and distilled water for 5 min; after a final rinse with 95% alcohol, it was air-dried at room temperature [25]. For antiserum coating, the gold electrodes were treated with 2.5% glutaraldehyde (0.5 μl) for 15 min, washed briefly with distilled water, and then dried. 2 μl of 100-fold diluted antiserum was applied to the pretreated gold electrode and incubated in a humid hood for 20 min. For the preparation of control QCMs, bovine serum albumin (BSA; 1 mg ml^{-1}, 0.5 μl) was applied instead. The coated electrodes were washed thoroughly with double-distilled water, followed by a PBS wash. Blocking was achieved by adding BSA (1 mg ml^{-1}, 0.5 μl), incubating in a humid hood for 1 h, washing with water, and rinsing with PBS. The coated QCM was assembled in a flow cell through which PBS was passed at a flow rate of 0.1 ml h^{-1}. The frequencies of all QCMs were monitored until steady state conditions were achieved (usually 30 min to 1 h).

The antibody-coated electrode was regenerated by 50 μl injection of 0.1 N HCl followed by a 10 min Milli-Q water wash. Repeated regeneration caused a decrease in binding capacity. The coated electrode could be regenerated five times for optimal detection. The crystal was repeatedly coated, cleaned, and washed until the gold electrode fell off. The repeated regeneration of electrodes caused a variation in the frequency response. Additionally, we observed a significant difference in the frequency response between different QCMs within the same batch.

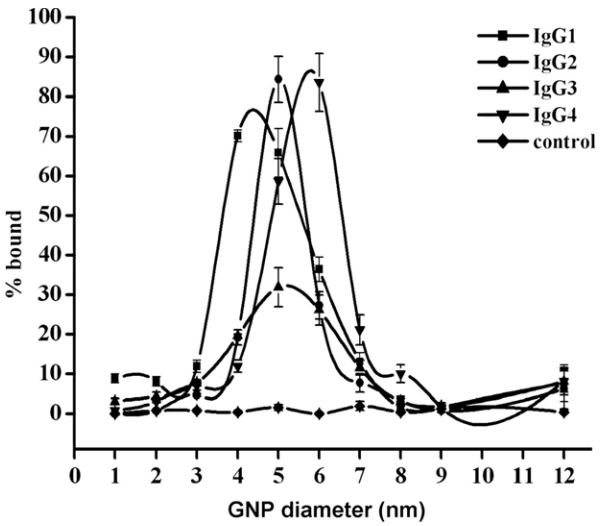

Figure 1. ELISA of anti-GNP antisera against various sizes of GNPs. Sera were obtained from mice immunized with 4 nm GNPs (IgG1, ■), 5 nm GNPs (IgG2, ●; IgG3, ▲), 6 nm GNP (IgG4, ▼), and control (♦). The percentage binding was calculated from the maximum binding of the 5 nm GNP-coated QCM as 100% and the background binding as 0%.

3. Results and discussion

3.1. Characterization of anti-GNP antisera

Antisera were obtained by immunizing mice with 4, 5, and 6 nm GNPs. The binding activity of antiserum against GNPs was verified by ELISA. We used GNPs ranging from 2 to 12 nm as the substrate to survey the binding activity against anti-4 nm GNP (IgG1), anti-5 nm GNP (IgG2 and IgG3), and anti-6 nm GNP (IgG4) antisera (figure 1). As expected, for IgG1, the binding activity peaked at 4 nm. For IgG2 and IgG3, the binding activity peaked at 5 nm. For IgG4, the binding activity peaked at 6 nm. The binding profiles exhibited as peaks with line widths of 2.7, 1.6, 3.1, and 2.0 nm for IgG1, IgG2, IgG3, and IgG4, respectively. It is interesting to note that the intensity of the peak reflected the binding affinity and relative concentration of immunoglobulin contained in the antisera. The line width of the binding profile indicated the range of GNPs that could be recognized by immunoglobulins, and thus is the selectivity of the antiserum.

Competition ELISA was performed to validate the binding selectivity of antiserum using 5 nm GNPs and 5 nm ZnO as competitors (data not shown). The binding activity was blocked in the presence of 5 nm GNPs but was undisturbed in the presence of 5 nm ZnO. The result indicated that antisera specifically bound to the gold surface and to a specific size of GNPs.

3.2. Biosensor that detects gold nanoparticles

A single QCM electrode was coated with anti-GNP antiserum and housed in a QCM-FIA system (figure 2). Coating of IgG2 was performed at five-fold saturation titer overnight to ensure maximum binding capacity. The detection of GNPs of different sizes was monitored by the frequency shift (figure 3). The injection of 1 mg ml^{-1} bovine serum albumin (BSA) and 1 mM ZnO did not induce a frequency change. The injection of 0.1 mM 5 nm GNPs induced a 21.6 Hz frequency shift. The injection of 3.5 nm GNPs induced a 5.3 Hz frequency shift. The injection of 8 nm GNPs induced a 0.8 Hz frequency shift. The injection of 12 and 37 nm GNPs did not induce any detectable frequency response. The immobilized anti-5 nm GNP antiserum was capable of detecting GNPs with

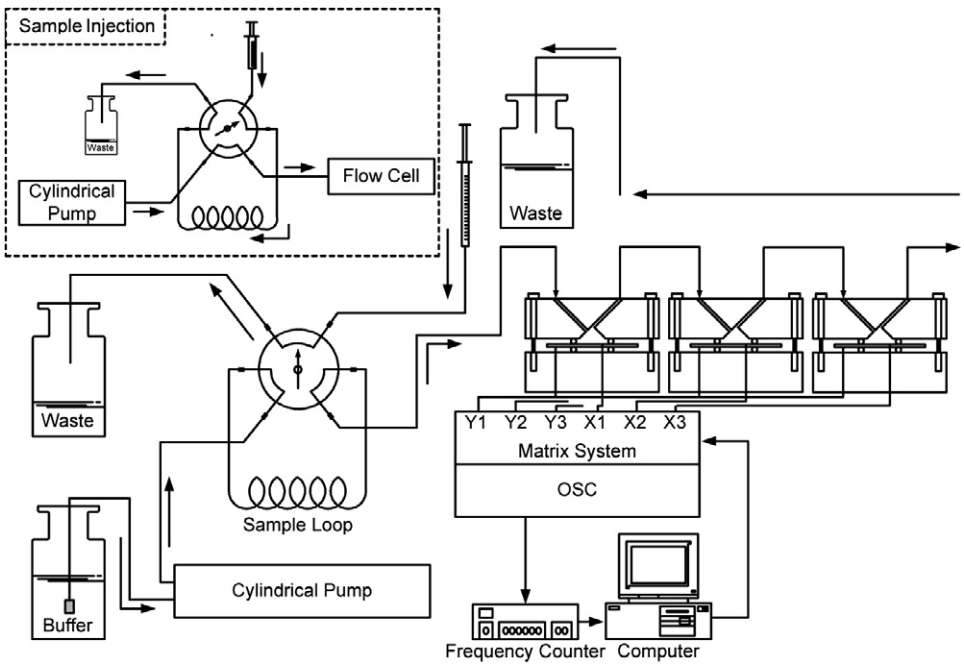

Figure 2. Scheme for the QCM flow injection analysis apparatus. Continuous flow was achieved using a cylindrical pump. The sample was injected through an injection loop and pumped into the array consisting of multiple flow cells.

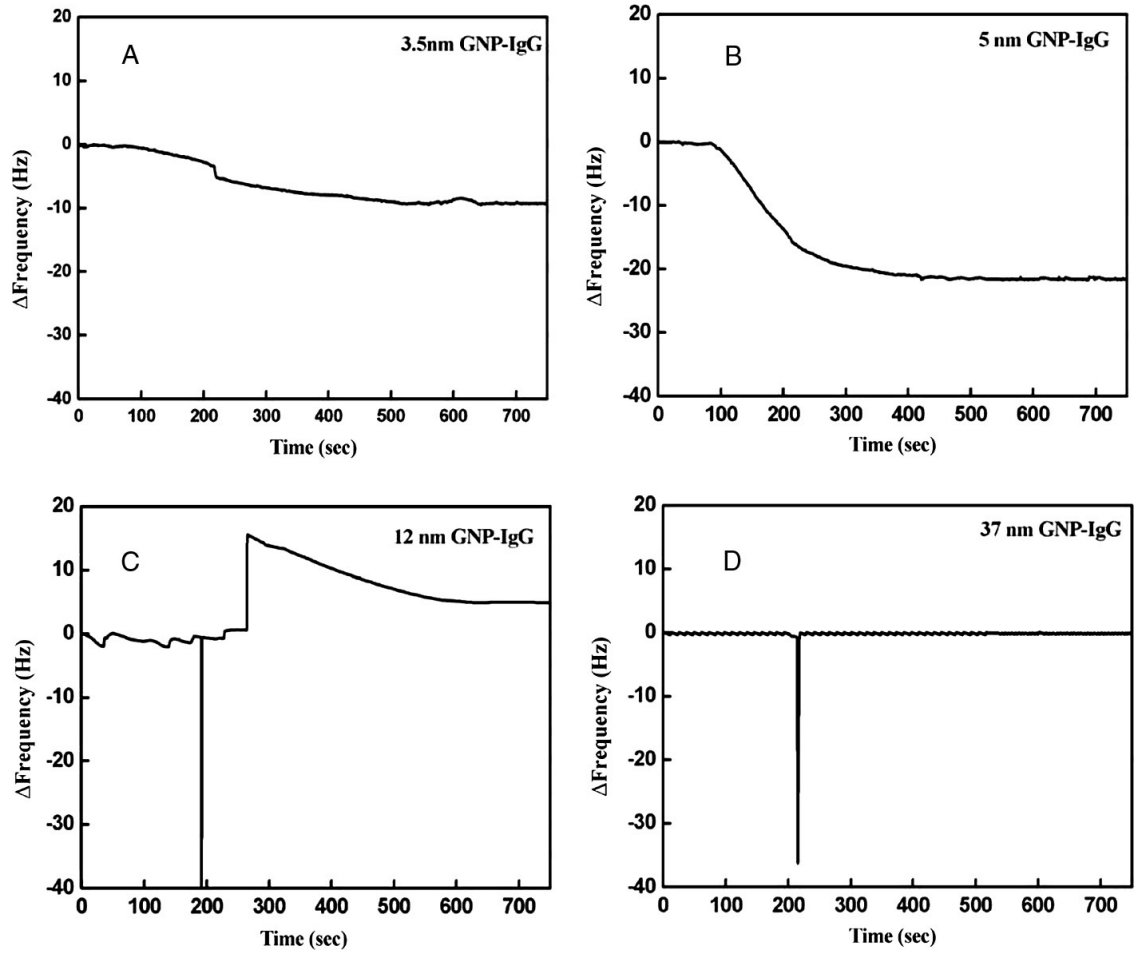

Figure 3. Detection of GNPs using an anti-5 nm GNP antiserum-coated QCM. The frequency shift was monitored for injection of 5 μl of (A) 3.5 nm GNPs, (B) 5 nm GNPs, (C) 12 nm GNPs, and (D) 37 nm GNPs. The concentration of GNPs was 0.1 mM. The switching action of the injector occasionally caused spikes during the detection.

differential affinity which maximized at 5 nm as expected from ELISA. The sensitivity for the detection of 5 nm GNPs was 10.3 ± 0.9 ng Hz^{-1}, with the low limit of detection at 5.5 ng.

Coating QCMs with other antisera was also performed. GNPs ranging from 2 to 12 nm were injected in sequence to obtain the binding affinity to each coated QCM. The binding reaction for each antiserum-coated QCM was analogous to previous ELISA results (figure 4). The binding activity peaked at 4.4 nm for IgG1, 5.2 nm for IgG2, 5.4 nm for IgG3, and 5.9 nm for IgG4. The line widths are 2.1, 1.8, 3.7, and 2.8 nm for IgG1, IgG2, IgG3, and IgG4, respectively. A minor shift in the peak position and binding efficiency was observed with IgG1 and IgG2, probably due to insufficient regeneration between injections.

The selectivity of the GNP sensor was verified by injecting various nanoparticles. These include TiO_2 (5 nm), ZnO (5 nm), and Fe_3O_4 (5 nm). Injections included TiO_2, ZnO, Fe_3O_4, GNPs, TiO_2/ZnO, TiO_2/Fe_3O_4, TiO_2 /GNPs, ZnO/Fe_3O_4, ZnO/GNPs, and Fe_3O_4/GNPs (figure 5). A different frequency shift was observed in the presence of ZnO and Fe_3O_4 in comparison to experiments in which the injection contained only GNPs.

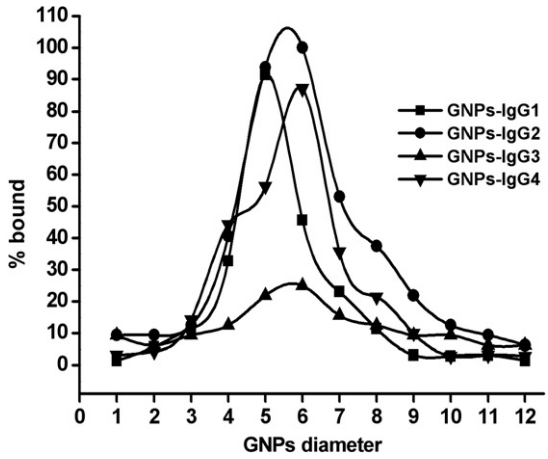

Figure 4. Detection of GNPs using an anti-GNP antiserum-coated QCM. The QCM electrode was coated with IgG1, IgG2, IgG3, or IgG4 antiserum and placed in the flow cell. The frequency shift was monitored for injection of 5 μl of various sizes of GNP, from 2 up to 12 nm. The electrode was regenerated between injections. The electrode was regenerated by 50 μl injection of 0.1 N HCl followed by a 10 min Milli-Q water wash. The percentage binding was calculated from the maximum binding of the 5 nm GNP-coated QCM as 100% and the background binding as 0%.

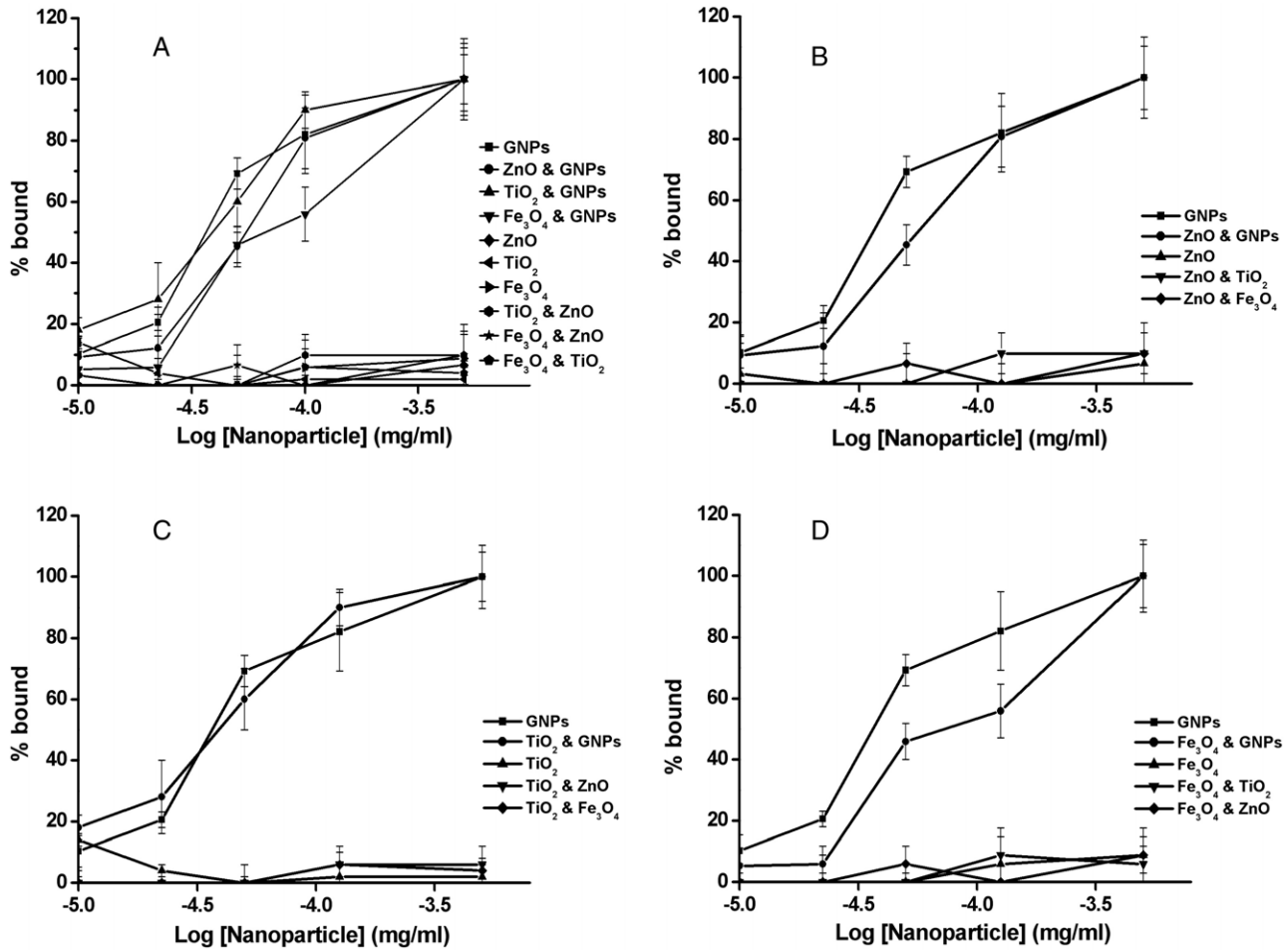

Figure 5. Injection of nanoparticles/GNP mixtures to the IgG2-coated QCM sensor. The QCM electrode was coated with IgG2 antiserum and placed in the flow cell. The frequency shift was monitored for injection of 5 μl of nanoparticles (GNPs, 5 nm; TiO_2, 5 nm; ZnO, 5 nm; and Fe_3O_4, 5 nm). For the injection of mixed nanoparticles, the concentration of GNPs is identical to that of the added nanoparticles as indicated by the X-axis. The electrode was regenerated between injections. The frequency shift was converted to percentage binding based on the maximum binding of each experiment. (A) Detection of GNPs, TiO_2, ZnO, Fe_3O_4, ZnO/GNPs, TiO_2/GNPs, Fe_3O_4/GNPs, TiO_2/ZnO, Fe_3O_4/ZnO, and Fe_3O_4/TiO_2. (B) Detection of GNPs, ZnO, ZnO/GNPs, TiO_2/ZnO, and Fe_3O_4/ZnO. (C) Detection of GNPs, TiO_2, TiO_2/GNPs, TiO_2/ZnO, and Fe_3O_4/TiO_2. (D) Detection of GNPs, Fe_3O_4, Fe_3O_4/GNPs, Fe_3O_4/ZnO, and Fe_3O_4/TiO_2.

The sensitivity of the antibody-coated QCM is approximately in the nanogram range, which is limited by the intrinsic detection limit of the piezoelectric sensor. The antibody-based detection is versatile and can be readily adapted to a variety of detecting platforms. Thus, the sensitivity for immunoglobulin-based detection can be improved by conjugating to a more sensitive platform, such as SPR or a nanowire. Although a further survey for various compounds will be required to elicit the selectivity of the current method, the extraordinary selectivity is expected based on the selectivity of antibody–antigen binding (figure 5). However, in figures 5(B) and (D) the addition of ZnO and Fe_3O_4 produced a significant downshift in comparison with GNPs alone. Because both the number of particles and the surface area for ZnO or Fe_3O_4 are not the same as for the same mass of GNP, it is likely that the downshift corresponds to the increase in number of particles or surface area. The increase in hydrophobic interaction might induce nonspecific binding between the immunoglobulin and the nanoparticles.

4. Conclusions

The current study has provided, for the first time, a platform for detecting nanoparticles in a convenient and economical manner. Since the existence of nanoparticles in our environment has already attracted substantial attention due to their possible toxic impact on biological systems, field detection of nanoparticles is becoming a technology that will be much in need. An immunoglobulin-based nanoparticle sensor thus provides a direct and economical solution.

Acknowledgments

This study was supported in part by the National Science Council in Taiwan (grants NSC96-2320-B-009-001 and NSC 97-2320-B-009-002-MY3) and the Bureau of Animal and Plant Health Inspection and Quarantine Council of Agriculture in Taiwan (grants 95AS-13.3.1-BQ-B1 and 95AS-13.3.1 -BQ-B6).

References

[1] van Dijk M A, Tchebotareva A L, Orrit M, Lippitz M, Berciaud S, Lasne D, Cognet L and Lounis B 2006 *Phys. Chem. Chem. Phys.* **8** 3486–95
[2] Hartland G V 2004 *Phys. Chem. Chem. Phys.* **6** 5263–74
[3] Hillenbrand R and Keilmann F 2001 *Appl. Phys.* B **73** 239–43
[4] Ignatovich F V and Novotny L 2003 *Rev. Sci. Instrum.* **74** 5231–5
[5] Ignatovich F V, Topham D and Novotny L 2006 *IEEE J. Sel. Top Quantum Electron.* **12** 1292–300
[6] Lindfors K, Kalkbrenner T, Stoller P and Sandoghdar V 2004 *Phys. Rev. Lett.* **93** 037401
[7] Seydack M 2005 *Biosens. Bioelectron.* **20** 2454–69
[8] Voisin C, Del Fatti N, Christofilos D and Vallee F 2001 *J. Phys. Chem.* B **105** 2264–80
[9] Dulkeith E, Niedereichholz T, Klar T A, Feldmann J, von Plessen G, Gittins D I, Mayya K S and Caruso F 2004 *Phys. Rev.* B **70** 205424
[10] Lee K L, Lee C W, Wang W S and Wei P K 2007 *J. Biomed. Opt.* **12** 044023
[11] Link S and El-Sayed M A 1999 *J. Phys. Chem.* B **103** 4212–7
[12] Haes A J and Van Duyne R P 2002 *J. Am. Chem. Soc.* **124** 10596–604
[13] Hong X and Kao F J 2004 *Appl. Opt.* **43** 2868–73
[14] Lamprecht B, Schider G, Lechner R T, Ditlbacher H, Krenn J R, Leitner A and Aussenegg F R 2000 *Phys. Rev. Lett.* **84** 4721–4
[15] Malinsky M D, Kelly K L, Schatz G C and Van Duyne R P 2001 *J. Am. Chem. Soc.* **123** 1471–82
[16] Sato Y, Sato K, Hosokawa K and Maeda M 2006 *Anal. Biochem.* **355** 125–31
[17] Zayats M, Kharitonov A B, Pogorelova S P, Lioubashevski O, Katz E and Willner I 2003 *J. Am. Chem. Soc.* **125** 16006–14
[18] Felidj N, Aubard J, Levi G, Krenn J R, Hohenau A, Schider G, Leitner A and Aussenegg F R 2003 *Appl. Phys. Lett.* **82** 3095–7
[19] Gunnarsson L, Bjerneld E J, Xu H, Petronis S, Kasemo B and Kall M 2001 *Appl. Phys. Lett.* **78** 802–4
[20] Jana N R 2003 *Analyst* **128** 954–6
[21] Schwartzberg A M, Grant C D, Wolcott A, Talley C E, Huser T R, Bogomolni R and Zhang J Z 2004 *J. Phys. Chem.* B **108** 19191–7
[22] Hwang W M, Lee C Y, Boo D W and Choi J G 2003 *Bull. Korean Chem. Soc.* **24** 684–6
[23] Malaquin L, Vieu C, Martinez C, Steck B and Carcenac F 2005 *Nanotechnology* **16** S240–5
[24] Huang G S, Chen Y S and Yeh H W 2006 *Nano Lett.* **6** 2467–71
[25] Huang G S, Wang M T and Hong M Y 2006 *Analyst* **131** 382–7
[26] Brown K R, Walter D G and Natan M J 2000 *Chem. Mater.* **12** 306–13
[27] Chithrani B D, Ghazani A A and Chan W C W 2006 *Nano Lett.* **6** 662–8
[28] Engvall E and Pearlmann P 1971 *Immunochemistry* **8** 871–4
[29] Holmgren J and Svennerholm A M 1973 *Infect. Immun.* **7** 759–63